

Evolution of a Stress-Driven Pattern in Thin Bilayer Films: Spinodal Wrinkling

Pil J. Yoo and Hong H. Lee*

School of Chemical Engineering, Seoul National University, Seoul, 151-744, Korea

(Received 22 April 2003; published 10 October 2003)

We report the full spectrum of the evolution of the wrinkle pattern formation in a thin bilayer film of an elastic metal on a viscoelastic polymer. Although the origin is different, the transition of an initial islandlike pattern to a labyrinthine structure without any change in the wavelength ($q \sim t^0$) and the overall evolutionary process is strikingly similar to that in the spinodal system but the process is robust and takes place on a long time scale (about 10 days). The change into a mountainous topography in the late stages is accompanied by an increase in the length scale from an initial wavelength to another. This change, due to the relaxation of the confined polymer that results in a transition from elastic- to viscouslike behavior, induces wave coarsening ($q \sim t^{-1.04 \pm 0.08}$) and macroscopic roughening.

DOI: 10.1103/PhysRevLett.91.154502

PACS numbers: 47.54.+r, 46.32.+x, 68.55.-a

Wrinkle formation in layered systems is a well known phenomenon and believed to take place spontaneously by an abrupt compressive stress [1,2]. A few approaches have been taken to examine the dynamics. One is an instability approach based on beam mechanics [3]. Another utilizes molecular dynamics simulations to describe the pattern coarsening process [4]. In these studies [2–4], the compressive stress due to the misfit strain is the driving force that is caused by a mismatch in the thermal expansion coefficient.

The bilayer system being considered is a thin polymer layer capped with a thin metal layer. The stress on the metal layer is generated upon heating the bilayer, which is tensile. As such, the metal surface would fracture once the stress exceeds its critical value if a simple expansion occurs in the polymer layer due to its larger thermal expansion coefficient. Our experimental results show, however, that an isotropically wrinkled surface results instead of a fractured surface, indicating that the viscoelastic property of the polymer induces an instability and makes the polymer deform in a vertical direction in relieving thermal stress.

Bilayers of aluminum on polystyrene (PS) were used in our experiments. Typically, a toluene solution of PS (high molecular weight: $M_n = 1\,340\,000$, $M_w/M_n = 1.05$, Polymer Source Inc.) was spin coated onto a silicon substrate, on which aluminum was thermally deposited to a desired thickness. For wrinkle formation, the prepared samples were placed in a constant-temperature oven and annealed for a period of time. The samples were then removed one at a time to examine the temporal evolution of wavy surface structure by atomic force microscopy (AFM, Digital Instruments, Dimension 3100) in the contact mode. Most of the experiments were carried out at 140 °C, well above the glass transition temperature of about 105 °C of the high molecular weight PS and some at 170 °C.

Temporal evolution of the surface pattern thus obtained experimentally is shown in Fig. 1 under set I [Figs. 1(a)–

1(f)] for a relatively small wave and those for a relatively large wave under set II [Figs. 1(g)–1(l)]. There are two distinct transitions in both sets regardless of the wave size under isothermal conditions. One is the transition from an islandlike to a labyrinthine pattern, as apparent in going from Fig. 1(a) to 1(b) in set I and Fig. 1(g) to 1(h) in set II. The formation of the islandlike structure is relatively fast, usually taking place in the first 3 min of annealing time. The evolution of the labyrinthine pattern to a more ordered structure takes a long time, usually more than a few days. Whether the pattern is islandlike or labyrinth, this early stage, which is to be called stage I, is characterized by the constancy of the dominant wave number of maximum intensity, q_m . The other transition is marked by the appearance of a second wave, as typified in the fast Fourier transforms (FFTs) of Figs. 1(d) and 1(i), i.e., the emergence of a second ring or a larger wave than the first in stage I. As time progresses, the larger wave starts exerting itself and becomes dominant over the initial wave. This period is to be called stage II.

The transition from an islandlike to a labyrinthine pattern is detailed in Fig. 2. The islandlike pattern is seen to evolve to a textured, to a partially developed labyrinthine, and to a fully developed labyrinthine pattern in about one day. The sectional data and mean roughness value (RMS) in the insets show that wave amplifies continuously, while the wavelength remains the same. The transition from a disordered islandlike to an ordered labyrinthine pattern can be quantitatively described by a disorder function [5]. The facts that waves grow with time but increase only in the magnitude, which is strain in wrinkling, without any change in the wavelength and the initial emergence of perturbational islandlike fluctuation are similar to those found in the early stage of spinodal decomposition [6,7]. However, the time it takes to establish an early stage in spinodal decomposition is so short that the dynamics are analyzed only in the reciprocal Fourier space and rarely captured in experiments [8]. In contrast, the stress-driven wrinkling in our system takes a

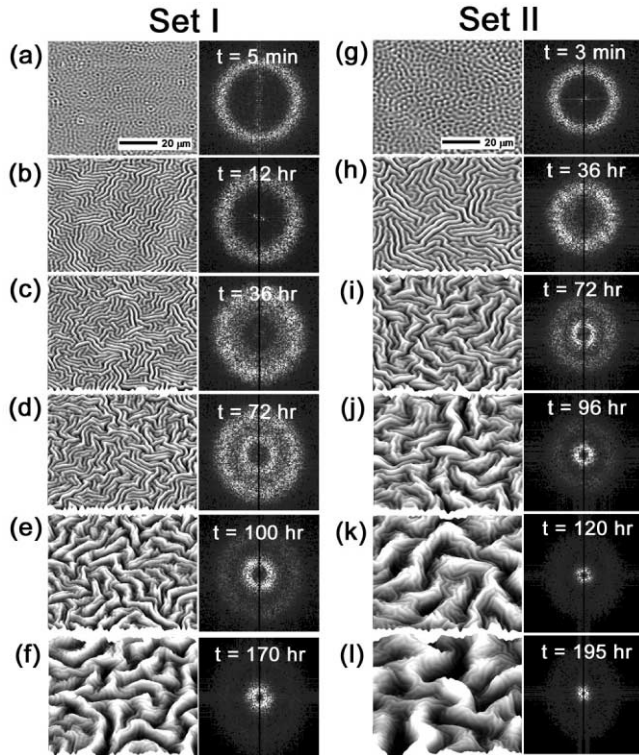


FIG. 1. AFM images of the temporal evolution of stress-driven surface wavy patterns ($80 \mu\text{m} \times 80 \mu\text{m}$). Set I (a)–(f) is for smaller waves that result in a thin metal layer (40 nm) and a relatively thin polymer layer (350 nm) and set II (g)–(l) is for larger waves that result when the polymer layer is made thicker (580 nm). Insets show the FFT images for given textured patterns. (a) Set I data after 3 min. (b) Set I data after 12 h. (c) Set I data after 36 h. (d) Set I data after 72 h. (e) Set I data after 100 h. (f) Set I data after 170 h. (g) Set II data after 3 min. (h) Set II data after 36 h. (i) Set II data after 72 h. (j) Set II data after 96 h. (k) Set II data after 120 h. (l) Set II data after 195 h.

long time to establish its early stage so that the slow and robust change of local behavior in surface pattern can be fully captured in experiment.

The constant intrinsic wavelength λ for stage I can be determined in an *a priori* manner [9]. The free energy per unit area of the metal/polymer bilayer system is given by

$$F(q) = \left[\frac{E_m q^2 t_m^3}{12(1 - \nu_m^2)} + \frac{E_p}{q^4 t_p^3} + \frac{2E_p}{3q} \right] \frac{(\varepsilon q)^2}{4}, \quad (1)$$

where t is the thickness, E is Young's modulus, the subscripts m and p are for the metal and the polymer, respectively, q is the wave number, ε is the amplitude of the wrinkling wave, and ν_m is the Poisson ratio of the metal. The first term represents the bending energy of the metal layer [10] and the second and third terms are the deformation energy of the underlying polymer layer in the long- and short-wavelength limit, respectively [11]. The usual approach for plate buckling with a viscous media does not take into account the viscoelastic properties of the underlying polymer layer [3,12]. The character-

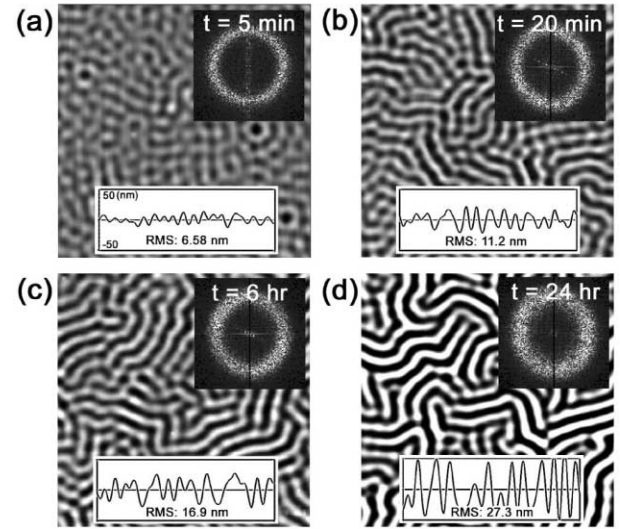


FIG. 2. AFM images of initial stage of wave development ($40 \mu\text{m} \times 40 \mu\text{m}$). The upper inset shows FFT for a given pattern and the lower inset gives sectional data and mean roughness value (RMS). (a) Islandlike pattern of set I data after 3 min of annealing. (b) Textured pattern of set I data after 20 min. (c) Weak labyrinthine pattern of set I data after 6 h. (d) Fully developed labyrinthine pattern of set I data after 24 h.

istic wavelength is determined by minimizing with respect to wave number the system free energy of the bilayer. The result predicts well the wavelength dependence on thickness and temperature variations. For instance, the theoretical values of the initial wavelength are 2.58 and 3.26 μm for set I and set II in Fig. 1, respectively, which compare with 2.45 and 3.08 μm from an experimental spectral data analysis.

By the time a labyrinthine pattern is completed in the early stage, a larger wave emerges as shown by the formation of two rings in the FFTs in Fig. 1, i.e., Figs. 1(d) and 1(i), signaling the beginning of stage II. The emergence of a second peak means that a new wavelength parameter intervenes and interacts with the initial wavelength. This characteristic can also be observed in other systems such as a Turing wave and spiral wave in chemical reactions [13] and a wave of composition fluctuation and that of capillary fluctuation in phase separation [14]. The dynamics of these two stages can be understood more precisely by an analysis of power spectra of the resulting patterns in Fig. 3(a). While the FFT images in Fig. 1 show that there exists one dominant large wave as indicated by a small ring near the center [Figs. 1(f) and 1(l)], the power spectra uncover the fact that initial waves are still retained even in the late stage. Thus, initial small waves are imbedded in the larger waves as in a mountainous topography [15]. However, once the second maximum peak emerges after about 36–48 h of annealing, the larger waves become dominant and get to grow with time.

A surprising finding in this Letter is that the strain of the metal layer remains constant even with increasing

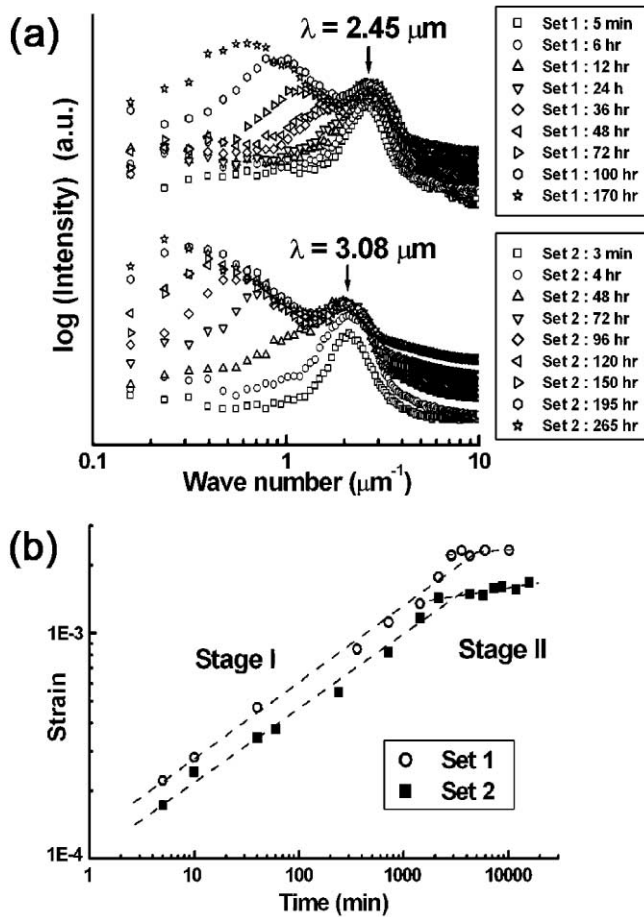


FIG. 3. (a) Power spectra intensity of evolving patterns as a function of wave number. Arbitrary unit is used for simultaneous representation of both sets I and II. Arrows indicate the maximum intensity peak of the pattern that formed on the surface initially. The second peak emerges with time and then become dominant in time. (b) Strain-time relation of metal layer. Strain-growth region corresponds to the early stage (stage I). The slope simply depends on material properties. In stage II, the strain is constant.

wavelength once the second larger wave emerges. It is very difficult to measure the strain of a thin metal layer (less than 100 nm) in the multilayer with a direct method. Instead, the surface area of the wrinkled surface was measured by AFM to calculate the strain indirectly. The change of the strain with time is shown in Fig. 3(b) for both stages. The plots show that in stage I, the strain increases with time but then becomes nearly constant when stage II starts. This type of behavior in strain-time relationship is the same as in creep and relaxation loading for the polymer [16]. The facts that no more stretching of metal takes place and the strain is independent of time in stage II suggest that the stress relaxation lies in the polymer layer.

For an analysis of stage II, we utilize the viscous property of polymer. The dynamic equation of motion for the bilayer can be expressed as follows [10,17]:

$$\frac{\partial}{\partial t} h(x, t) = C \frac{\partial^2 P}{\partial x^2} = C \frac{\partial^2}{\partial x^2} \left[\frac{E_m t_m^3}{12(1-\nu^2)} \frac{\partial^4 h}{\partial x^4} - \gamma \frac{\partial^2 h}{\partial x^2} \right], \quad (2)$$

where h is the local film thickness, x is the lateral coordinate, C is the constant that is dependent on the flow profile and the viscosity, P is the pressure, γ is the interfacial tension. For a small fluctuation of the film thickness, $h(x, t) = h_0 + \varepsilon \cos(qx) \exp(t/\tau)$, and Eq. (2), when the perturbation is introduced into the equation, yields

$$(C\tau)^{-1} = -\frac{E_m t_m^3}{12(1-\nu^2)} q^6 - \gamma q^4, \quad (3)$$

where τ is the growth parameter. The relationship leads to a stability condition that the wave number approach zero for the fastest growing wave, which means that the wavelength should continuously grow with time without bound. However, as the polymer layer thickness is finite, the wavy pattern becomes “pinned” after about 200–280 h of annealing. Therefore, the resulting wavelength is larger for thicker polymer layer. A sectional scanning electron micrograph (SEM) in Fig. 4(a) shows that the valleys of the wrinkles indeed reached the substrate surface, which confirms the pinning behavior.

Figure 4(b) shows the wave number plotted against time. As indicated earlier, the wave number remains the same in stage I. In stage II of interest here, it is seen that the wave number is inversely proportional to time (all experimental values from six data sets are in the range between -0.958 and -1.12). It is notable that this growth rate dependence is identical with that found in the late coarsening stage of spinodal decomposition [6,18].

A discussion is in order here on the similarities between the spinodal wrinkling in buckled bilayers and the spinodal decomposition in polymer blends. To start with, both phenomena are spinodal, which is an initiation of small perturbations with a certain wavelength, as is evident from Figs. 1(a) and 1(g). The initiation is by an instability in both, the former due to a thermomechanical instability that leads to a deflection wave due to a surface deformation, and the latter due to a thermodynamic one that leads to a composition wave due to a phase separation. With the strain as the magnitude of wave in wrinkling, there is a one to one correspondence between the stages of the wrinkling and those of the decomposition. In both cases, the wavelength is constant but the magnitude increases with time in the early stage. In the late stage, the wavelength increases with time but the magnitude stays constant. Although there is no stage in the wrinkling that corresponds to the intermediate stage of the decomposition, the mechanism responsible for the process leading up to the saturation is similar and in this context, stage I corresponds to a combination of the early and intermediate stages of the decomposition. In the spinodal decomposition, the magnitude keeps increasing but eventually

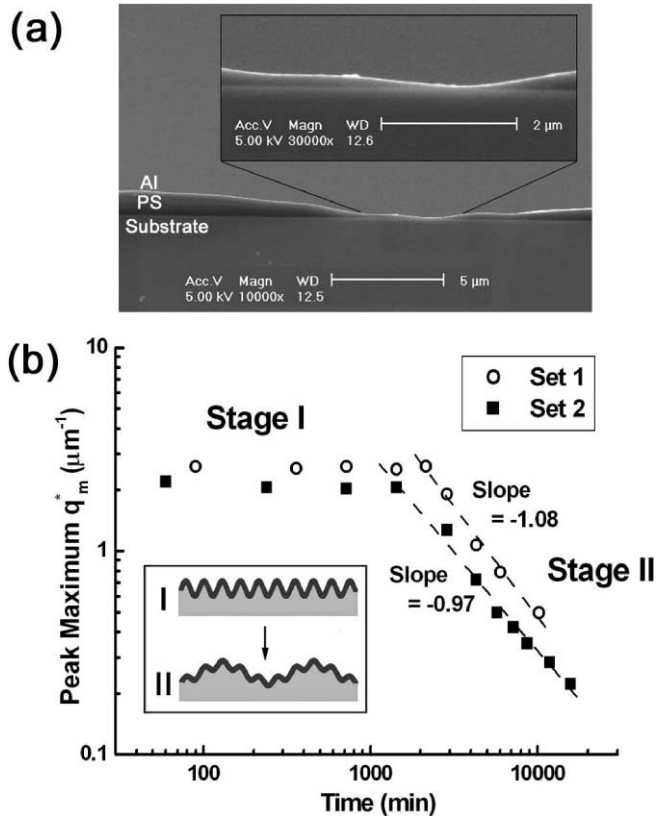


FIG. 4. (a) SEM micrograph for verification of “pinned” wave after 280 h of annealing in set II. The inset is a magnified image of the “pinned” region. One can observe that one half of one large wave (viscosity-induced wave) is composed of four small waves (elasticity-induced wave) as seen in Fig. 1(l). (b) Dominant wave number-time relation in stages I and II. The wavelength is constant during stage I but increases almost linearly with time in stage II.

reaches a saturation value that corresponds to the maximum composition gradient. While the driving force in the decomposition is composition gradient, it is stress in the wrinkling. In the wrinkling, the magnitude also keeps increasing but eventually reaches a saturation value that corresponds to the maximum stress. The saturation corresponding to the maximum driving force marks the beginning of the late stage in both cases. The mechanism involved in the growth of the wavelength is coarsening in both. The coarsening in spinodal decomposition is viscosity controlled [19] and so is the coarsening in spinodal wrinkling. Therefore, the exponent of the time dependence of the wavelength growth is unity for both spinodal decomposition and spinodal wrinkling.

In summary, spinodal wrinkling can be characterized as one in which the wavelength remains constant and the strain increases with time in stage I (elasticity induced wave), but the strain remains constant in stage II (viscosity induced wave) while the wavelength increases with time.

This work was supported by Korea Research Foundation Grant (No. KRF-2002-041-D00346).

*To whom correspondence should be addressed.

Email address: honghlee@snu.ac.kr

- [1] S. P. Timoshenko and J. M. Gere, *Theory of Elastic Stability* (McGraw-Hill, New York, 1961); J. W. Hutchinson and Z. Suo, *Adv. Appl. Mech.* **29**, 63 (1992); G. Gioia and M. Ortiz, *Adv. Appl. Mech.* **33**, 119 (1997).
- [2] N. Bowden *et al.*, *Nature (London)* **393**, 146 (1998); N. Bowden, W. T. S. Huck, K. E. Paul, and G. M. Whitesides, *Appl. Phys. Lett.* **75**, 2557 (1999); D. B. H. Chua, H. T. Ng, and S. F. Y. Li, *Appl. Phys. Lett.* **76**, 721 (2000).
- [3] N. Sridhar, D. J. Srolovitz, and Z. Suo, *Appl. Phys. Lett.* **78**, 2482 (2001); R. Huang and Z. Suo, *J. Appl. Phys.* **91**, 1135 (2002).
- [4] L. Golubovic, D. Moldovan, and A. Peredera, *Phys. Rev. Lett.* **81**, 3387 (1998); D. Moldovan and L. Golubovic, *Phys. Rev. Lett.* **82**, 2884 (1999).
- [5] G. H. Gunaratne, A. Ratnaweera, and K. Tennekone, *Phys. Rev. E* **59**, 5058 (1999); G. H. Gunaratne, R. E. Jones, Q. Ouyang, and H. L. Swinney, *Phys. Rev. Lett.* **75**, 3281 (1995).
- [6] J. W. Cahn, *Trans. Metall. Soc. AIME* **242**, 166 (1968); K. Binder, in *Materials Science and Technology*, edited by R. W. Cahn, P. Haasen, and E. J. Kramer (VCH, New York, 1991), Vol. 5; F. S. Bates and P. Wiltzius, *J. Chem. Phys.* **91**, 3258 (1989).
- [7] G. Reiter, *Phys. Rev. Lett.* **68**, 75 (1992); A. M. Higgins and R. A. L. Jones, *Nature (London)* **404**, 476 (2000).
- [8] S. Joly *et al.*, *Phys. Rev. Lett.* **77**, 4394 (1996).
- [9] P. J. Yoo, S. Y. Park, K. Y. Suh, and H. H. Lee, *Adv. Mater.* **14**, 1383 (2002).
- [10] L. D. Landau and E. M. Lifshitz, in *Theory of Elasticity* (Pergamon, Oxford, 1970).
- [11] G. H. Fredrickson, A. Ajdari, L. Leibler, and J. P. Carton, *Macromolecules* **25**, 2882 (1992).
- [12] N. Sridhar, D. J. Srolovitz, and B. N. Cox, *Acta Mater.* **50**, 2547 (2002).
- [13] L. Yang, M. Dolnik, A. M. Zhabotinsky, and I. R. Epstein, *J. Chem. Phys.* **117**, 7259 (2002); R. Kapral and K. Showalter, *Chemical Waves and Patterns* (Kluwer Academic, Dordrecht, 1994).
- [14] H. Wang and R. J. Composto, *Macromolecules* **35**, 2799 (2002).
- [15] P. Ball, *The Self-Made Tapestry* (Oxford, New York, 2001); M. C. Cross and P. C. Hohenberg, *Rev. Mod. Phys.* **65**, 851 (1993).
- [16] A. S. Wineman and K. R. Rajagopal, *Mechanical Response of Polymers* (Cambridge, New York, 2000).
- [17] S. Herminghaus, *Phys. Rev. Lett.* **83**, 2359 (1999); K. Y. Suh and H. H. Lee, *Phys. Rev. Lett.* **87**, 135502 (2001).
- [18] M. Joshua, J. V. Maher, and W. I. Goldberg, *Phys. Rev. Lett.* **51**, 196 (1983); J. Y. Kim *et al.*, *Phys. Rev. Lett.* **71**, 2232 (1993); L. Sung, A. Karim, J. F. Douglas, and C. C. Han, *Phys. Rev. Lett.* **76**, 4368 (1996).
- [19] E. D. Siggia, *Phys. Rev. A* **20**, 595 (1979); H. Furukawa, *Physica (Amsterdam)* **204A**, 237 (1994).